Packing of ruthenium sensitizer molecules on mostly exposed faces of nanocrystalline TiO2: Crystal structure of (NBu4+)2[Ru(H2tctterpy)(NCS)3]2−.0.5DMSO

ARTICLE *in* APPLIED ORGANOMETALLIC CHEMISTRY · NOVEMBER 2002

Impact Factor: 2.25 · DOI: 10.1002/aoc.361 · Source: OAI

4 AUTHORS, INCLUDING:

Valery Shklover
ETH Zurich
348 PUBLICATIONS **6,607** CITATIONS
SEE PROFILE

Md Khaja Nazeeruddin
École Polytechnique Fédérale de Lausanne
489 PUBLICATIONS **45,050** CITATIONS
SEE PROFILE

APPLIED ORGANOMETALLIC CHEMISTRY
Appl. Organometal. Chem. 2002; **16**: 635–642
Published online in Wiley InterScience (www.interscience.wiley.com). DOI:10.1002/aoc.361

Packing of ruthenium sensitizer molecules on mostly exposed faces of nanocrystalline TiO_2: crystal structure of $(NBu_4^+)_2[Ru(H_2tctterpy)(NCS)_3]^{2-}\cdot 0.5\,DMSO$

V. Shklover[1]*, Md. K. Nazeeruddin[2], M. Grätzel[2] and Yu. E. Ovchinnikov[1]

[1]Laboratory of Crystallography, Swiss Federal Institute of Technology, CH-8092 Zürich, Switzerland
[2]Institute of Photonics and Interfaces, Department of Chemistry, Swiss Federal Institute of Technology, CH-1015 Lausanne, Switzerland

Received 25 March 2002; Accepted 18 July 2002

An X-ray crystal study of the new 'black dye' sensitizer tri(thiocyanato)(4,4′,4″-tricarboxy-2,2′:6′,2″-terpyridine)ruthenium(II) is reported. In the crystal, strong hydrogen bonds form chains of ruthenium complex dianions with the O···O distances of 2.48–2.54 Å. From the molecular geometry of the dianions, structural models of their close packing on the (101) and (001) crystal surfaces of TiO_2 (anatase) have been built. The maximum possible density of molecular packing noticeably exceeds the experimental value. The hydrogen bonding between the anions in monolayers, located on the TiO_2 surface, is discussed. Copyright © 2002 John Wiley & Sons, Ltd.

KEYWORDS: ruthenium; bipyridinyl complexes; crystal structure; TiO_2 nanocrystals; absorbed monolayers

INTRODUCTION

Covering inorganic nanoparticles by various organic layers is now a normal method of obtaining desired physical properties of heterosystems.[1–5] Fine tuning of the properties may be achieved by changing the size and shape of nanoparticles,[6] their mutual arrangement,[7,8] and the thickness and surface density of organic layers.[9] In addition, interactions between surface molecules can also affect some physical characteristics of the system,[10] quite aside from their influence on the density of covering layers. Among possible interactions in the surface layers, hydrogen bonds (H-bonds) are of special interest because they may serve as a specific tool for layer formation or alternatively could play a negative role in this process, e.g. making the structure of this layer less dense.

Extensive investigations of pyridinyl ruthenium complexes, which are excellent sensitizers for the TiO_2 semiconductor in photovoltaic cells,[11] have been carried out in the last decade.[12–18] Adsorbed monolayers of these complexes are interesting as being representative of two-dimensional molecular structures modulated by strong chemical interactions. The various experimental techniques that may be applied in studying sensitized TiO_2 semiconductors, i.e. diffraction methods,[20–23] spectroscopy,[24] scanning and transmission electron microscopy,[25,26] or atomic force microscopy,[27] meet certain difficulties, since these methods require special preparation of the interface. On the other hand, a sufficiently rigid structure of absorbed molecules allows modeling of the molecular packing on the semiconductor crystal surface using molecular parameters obtained from X-ray crystal studies. We first applied this modeling method to bis[(4,4′-carboxy-2,2′-bipyridine)-(thiocyanato)] ruthenium(II) (henceforward referred to as N3) on the (101) crystal surfaces of anatase.[28] New experimental data[29] confirmed our essential assumptions and conclusions, proving the fruitfulness of the molecular modeling approach.

The presence of chemically active terminal groups, i.e. COOH (COO^-), is required to link pyridinyl ruthenium complexes with the semiconductor surface. These groups, however, have a strong inclination to form H-bonds, which can drastically affect the structure of the surface monolayer, and, moreover, could increase its thickness.

The new 'black dye' complex tri(thiocyanato)(4,4′,4″-tricarboxy-2,2′:6′,2″-terpyridine)ruthenium(II) has a very impressive electronic absorption spectra,[30] which proves its efficiency as a sensitizer. However, its monolayer surface concentration is essentially lower than that of the N3

*Correspondence to: V. Shklover, Laboratory of Crystallography, Swiss Federal Institute of Technology, CH-8092 Zürich, Switzerland.
E-mail: v.shklover@kristall.erdw.ethz.ch
Contract/grant sponsor: Swiss National Science Foundation; Contract/grant number: 7SUPJ062151.00/1.

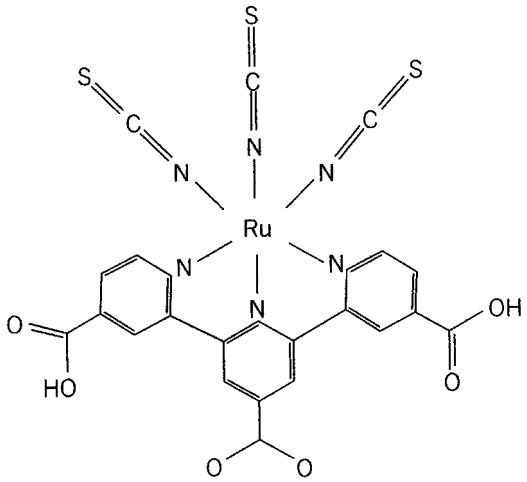

Figure 1. Chemical structure of dianion $[Ru(H_2tctterpy)(NCS)_3]^{2-}$ (**1**) (counterions are NBu_4^+).

complex investigated previously, in spite of the larger molecular size of the latter. The photocurrent through the TiO_2 surface sensitized with black dye is therefore diminished. To elucidate possible reasons for such behavior, we have determined the crystal and molecular structure of the diprotonated complex $(NBu_4^+)_2[Ru(H_2tctterpy)(NCS)_3]^{2-}$ ·0.5DMSO (**1**) and have built models of monolayers of its anions (Fig. 1) on the TiO_2 (anatase) crystal surface. The full structural report and analysis of these packing models is the subject of this paper.

EXPERIMENTAL

X-ray structure study of complex 1

The data collection for a single crystal of **1** was performed at 243 K on a Siemens SMART PLATFORM with CCD detector, using Mo K_α radiation, graphite monochromator, and the ω-scan technique with an exposure time of 120 s/frame. Other experimental details and results of the structure refinement are shown in Table 1. The hydrogen atoms were not localized, but in terpyridyl moieties they were placed in calculated positions and refined in a 'riding model' with fixed C—H distances and isotropic displacement parameters $U = 0.08$ Å^2. To diminish the effects of the very intense thermal motion of NBu_4 cations and dimethylsulfoxide (DMSO) molecules, locations of all the atoms of these molecules were refined isotropically with occupancies of 0.5. The groups with equivalent bond distances and bond angles in NBu_4 cations were refined as unique parameters with fixed 'inner' standard deviations (0.03 Å for bonds). During the refinement a twofold disorder of the sulfur atom in the DMSO molecule was revealed. Subsequent refinement gave occupancy factors of 0.4 and 0.6 for these positions, i.e. the DMSO molecule accepts two orientations with approximately equal probabilities.

Table 1. Crystal data and experimental details of X-ray structure study for $(NBu_4^+)_2[Ru(H_2tctterpy)(NCS)_3]^{2-}$ 0.5DMSO (**1**)

Formula weight	2327.16
Crystal color, habit	brown, plate
Crystal dimensions (mm^3)	0.0 × 0.3 × 0.15
Crystal system	Monoclinic
Space group	*Cc*
Lattice parameters	
a (Å)	32.141(6)
b (Å)	23.257(5)
c (Å)	23.365(5)
α (deg)	90
β (deg)	133.06(3)
γ (deg)	90
V (Å^3)	12761(5)
Z	8
Density calc. (g cm^{-3})	1.211
Absorption coefficient μ(Mo Kα) (mm^{-1})	0.41
Extinction coefficient	0.000 59(11)
$F(000)$	4936
θ range (deg) for data collection	1.23 to 20.81
Reflections collected/independent	19103/12073
Observed reflections, $I > 2\ \sigma\ (I)$	7731
Refinement method	Full-matrix least-squares on F^2
Data/restraints/parameters	12036/208/959
Goodness-of-fit on F^2	1.005
Final R_1, wR_2 indices [$I > 2\ \sigma(I)$]	0.0978, 0.2464
R_1, wR_2 indices (all data)	0.1452, 0.3003
Absolute structure parameter	0.40(7)

The coordinates of non-hydrogen atoms are listed in a separate table, which, along with other details of the X-ray study, has been deposited at the Cambridge Crystallographic Data Centre. The SHELX PLUS suite of programs[31] was used for data reduction, structure solution, and refinement.

RESULTS AND DISCUSSION

Crystal structure of complex 1

The asymmetric unit of the crystal structure of **1** contains two double-charged anionic ruthenium complexes, four NBu_4^+ cations, and the DMSO molecule. The conformations of the crystallographically independent anionic ruthenium complexes (Fig. 2) are the same within the accuracy of experimental error (Table 2). On the contrary, the conformations of all the NBu_4^+ cations are essentially different and, from the standpoint of packing (as space-filling bodies), they should be considered as different types of molecule.

The main feature of the crystal structure of **1** is a chain

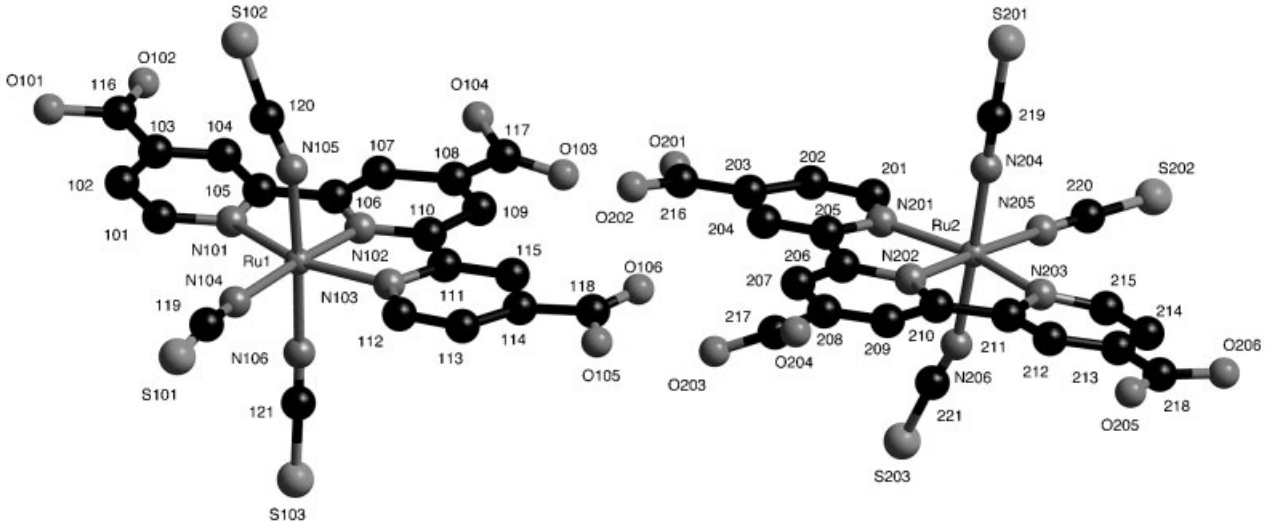

Figure 2. Structure of crystallographically independent anions **1**. Hydrogen atoms are not shown.

Table 2. Main bond lengths (Å) and bond angles (deg) in independent anions **1**

Ru(1)—N(101) 2.058(14)	Ru(2)—N(201) 2.090(14)
Ru(1)—N(102) 1.908(12)	Ru(2)—N(202) 1.936(14)
Ru(1)—N(103) 2.059(13)	Ru(2)—N(203) 2.033(13)
Ru(1)—N(104) 2.09(2)	Ru(2)—N(204) 1.90(3)
Ru(1)—N(105) 2.01(2)	Ru(2)—N(205) 2.03(2)
Ru(1)—N(106) 2.02(2)	Ru(2)—N(206) 2.05(2)
S(101)—C(119) 1.56(2)	S(201)—C(219) 1.69(3)
S(102)—C(120) 1.66(3)	S(202)—C(220) 1.67(2)
S(103)—C(121) 1.70(3)	S(203)—C(221) 1.61(3)
O(101)—C(116) 1.38(2)	O(201)—C(216) 1.31(2)
O(102)—C(116) 1.17(2)	O(202)—C(216) 1.22(2)
O(103)—C(117) 1.22(2)	O(203)—C(217) 1.27(2)
O(104)—C(117) 1.32(2)	O(204)—C(217) 1.24(2)
O(105)—C(118) 1.34(2)	O(205)—C(218) 1.24(2)
O(106)—C(118) 1.11(2)	O(206)—C(218) 1.26(2)
N(102)—Ru(1)—N(101) 78.8(5)	N(202)—Ru(2)—N(201) 81.0(7)
N(103)—Ru(1)—N(101) 159.2(5)	N(203)—Ru(2)—N(201) 161.5(6)
N(104)—Ru(1)—N(101) 104.8(6)	N(205)—Ru(2)—N(201) 101.3(6)
N(105)—Ru(1)—N(101) 86.0(6)	N(204)—Ru(2)—N(201) 91.9(7)
N(106)—Ru(1)—N(101) 91.7(6)	N(206)—Ru(2)—N(201) 85.9(6)
N(102)—Ru(1)—N(103) 80.6(5)	N(202)—Ru(2)—N(203) 80.4(6)
N(102)—Ru(1)—N(104) 176.1(6)	N(202)—Ru(2)—N(205) 177.5(6)
N(102)—Ru(1)—N(105) 92.6(6)	N(204)—Ru(2)—N(202) 89.4(8)
N(102)—Ru(1)—N(106) 88.4(6)	N(202)—Ru(2)—N(206) 91.8(7)
N(103)—Ru(1)—N(104) 95.8(6)	N(203)—Ru(2)—N(205) 97.2(6)
N(105)—Ru(1)—N(103) 92.4(6)	N(204)—Ru(2)—N(203) 88.2(8)
N(106)—Ru(1)—N(103) 90.3(6)	N(203)—Ru(2)—N(206) 94.4(7)
N(105)—Ru(1)—N(104) 89.0(6)	N(204)—Ru(2)—N(205) 91.3(8)
N(106)—Ru(1)—N(104) 90.1(6)	N(206)—Ru(2)—N(205) 87.6(7)
N(105)—Ru(1)—N(106) 177.2(6)	N(204)—Ru(2)—N(206) 177.3(7)

system formed by anions linked by the strong H-bonds (Fig. 3). These chains are one-dimensional, though the almost perfect coplanarity of the terpyridine planes in neighboring anions suggests that we can consider them as 'ribbons'. The ribbons extend along the [112] and [1$\bar{1}$2] crystal directions, and adjacent crystallographically independent anions are related by approximate inversion centers. So, the anionic ruthenium complex has its own approximate *mm* symmetry, and symmetrically independent anions have, in fact, the same conformation; the chain symmetry is rather high. The great variety of NBu_4^+ conformations (some butyl groups even have *gauche* configurations) arise apparently because of powerful cation···anion electrostatic interactions. Significant twisting of some COO(H) groups with respect to the terpyridinyl planes may also be noted: for the C(217)O(203)O(204) group the corresponding torsion angle reaches 29°. This feature is also observed in the crystal structure of N3,[28] and is apparently induced by intermolecular forces.

Hydrogen bonding

It is interesting to note that ruthenium complexes do not usually form dimers using carboxylic acids due to H-bonds of the COOH groups.[32] However, in the crystal of **1**, instead of monomers, we observe continuous rows of centrosymmetric pairs of molecules. Thus, in the crystal of **1** there are two donor (carboxylate) groups per four acceptor (carboxylic acid) groups. The electron acceptor oxygen atoms of half of the carboxylic groups are not involved. The packing in the ribbons is compact, and the two CO groups of each anion, which do not participate in H-bonds, are located in the shielded positions. As the ribbon does not have active groups to which external agents may adjoin, the polyanion chain has a certain stability. The low accuracy of the

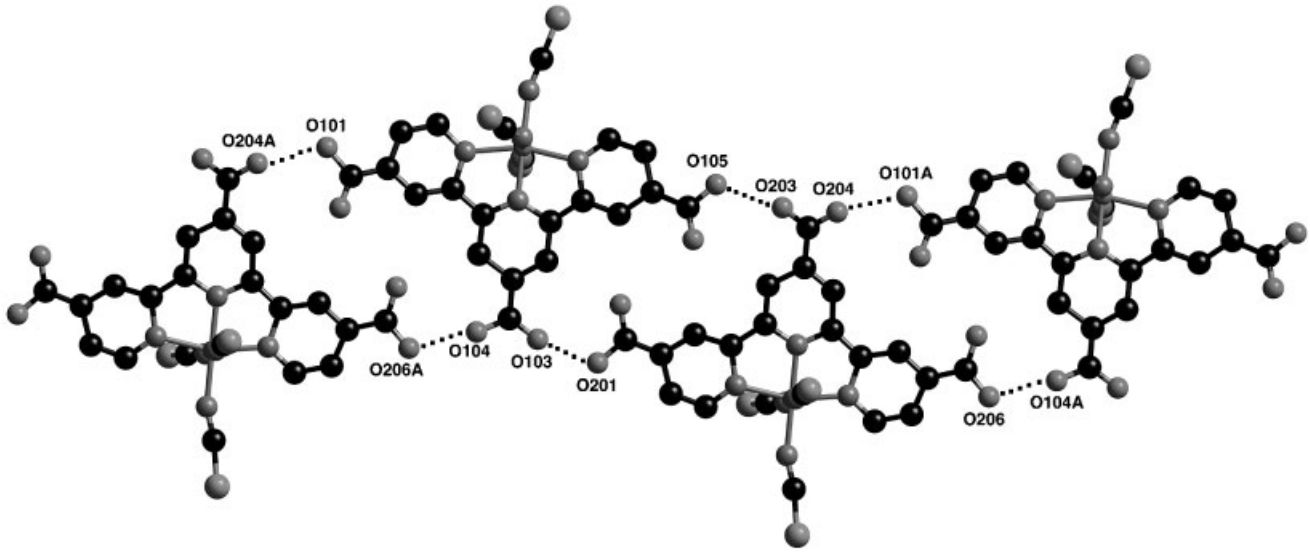

Figure 3. Structure of a polyanion chain in crystal **1** (projection on the mean plane of terpyridyl ligands). H-bonds are signed with dashed lines. The O···O distances are listed in Table 3.

geometrical parameters (Table 2) does not allow us to point out exact positions of the deprotonated COO^- groups. It is possible that the great displacement parameters of the oxygen atoms and the strong distortions of the usual geometry in these groups (see Table 2 and material, deposited of the Cambridge Crystallographic Data Centre) are explained by static disorder of protons over all possible positions in the H-bonds.

Taking this into account, a real value of *ca* 2.50 Å should be accepted for the O···O distances in the H-bonds (Table 3). According to the classification[33] such hydrogen bonds are 'strong' with an energy of *ca* 15 kcal mol^{-1} (~63 kJ mol^{-1}). However, having these parameters, the H-bonds are far from symmetric, and the above suggestion about static disorder is reasonable.

Possible models of the absorbed monolayer

According to our previous studies,[34–36] the (101) and (001) faces are the most exposed crystal surfaces in TiO_2 (anatase) nanofilms. Earlier, we have analyzed structural aspects of chemisorption on the (101) anatase crystal face for the neutral ruthenium complex N3 using general stereochemistry rules.[28] For a carboxylate group, the bridging coordination mode (Fig. 4) was found to be favored. With a distance of 3.78 Å between neighboring surface titanium atoms, the bond lengths and bond angles at the titanium, oxygen, and carbon 'bridging' atoms display a minimum steric distortion. This coordination model was recently confirmed experimentally with IR spectroscopy.[29] In their investigation, Wang *et al.*[37] showed that the HCOOH groups are found to attached onto the TiO_2 (rutile) surface as bridge between neighboring titanium atoms. Finnie et al.[29] suggested that the attachment of the COO group to a single titanium atom is also possible, although this would require heptacoordination for the surface titanium atom and would make the Ti—O bonds in the four-membered chelate cycle rather weak.

Table 3. Geometrical parameters of hydrogen bonds (Å) in crystal **1**

O(101)···O(204) $(0.5+x, 0.5+y, 1+z)$	2.58
O(103)···O(201)	2.41
O(104)···O(206) $(0.5+x, 0.5+y, 1+z)$	2.48
O(105)···O(203)	2.54
(O···O)(av.)	2.50

The structure of anion **1** (Fig. 2) allows anchoring to titanium atom of anatase nanoparticles with only one COO group. Thus, an anion of **1** may anchor to the (101) and (001) crystal faces of anatase in the two ways shown in Fig. 4 (B and C types, i.e. with the central or side-bridging COO group).

The essential difference between the adsorption states of the N3 and anion **1** complexes is in the degrees of freedom of the molecules. The N3 molecules, anchored by two COO groups, do not undergo significant thermal motion (except possible surface diffusion), whereas anion **1** can perform torsion oscillations around the O···O line of the anchoring COO group with an amplitude of 10° or even more; such oscillations do not cause significant changes in the bonding geometry of this group. Additionally, the attachment by a single COO group makes surface diffusion much easier.

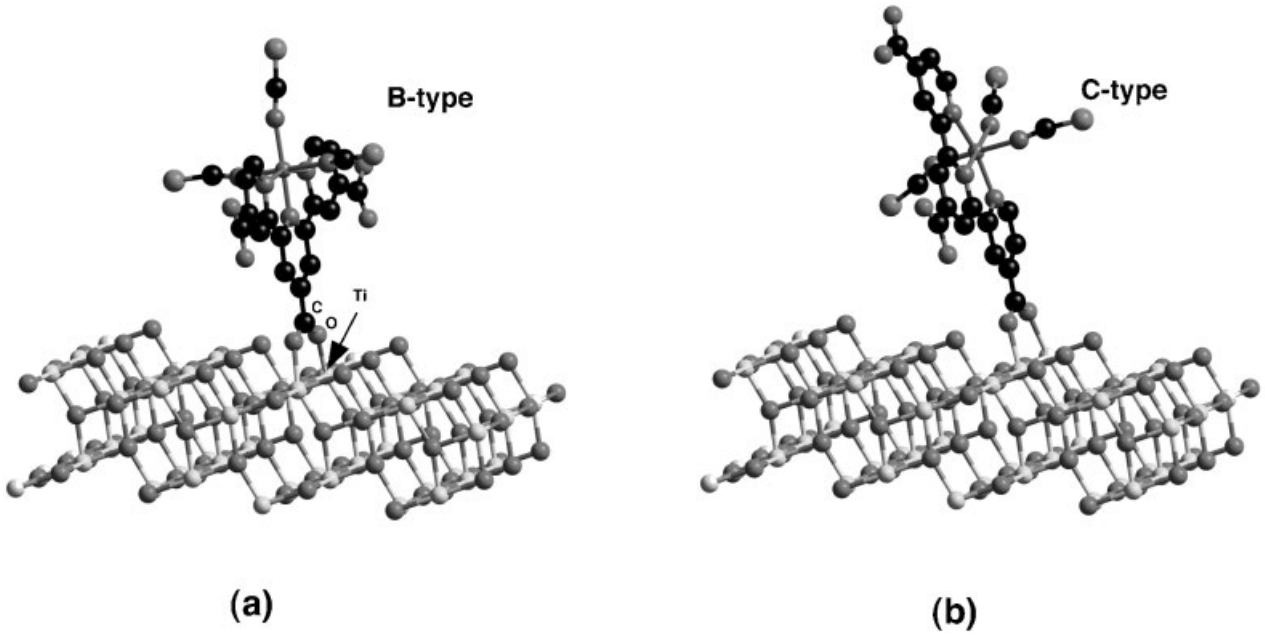

Figure 4. Possible types of anchoring of anions **1** to the (101) anatase surface: (a) with an axial COO group; (b) with a side COO group. Anchoring to the (001) surface has a similar geometry.

These peculiarities, in principle, enable anions **1** to pack more tightly; in condition, they could also facilitate formation of hydrogen bonds within the monolayer.

The exact structure of the monolayer, however, is determined essentially by the arrangement of chemisorption sites, i.e. the pentacoordinated surface titanium atoms, on the TiO_2 surface. The (101) and (001) crystal faces of anatase are different in that respect. The (101) has a rectangular centred unit cell [3.78, 10.23] Å, which contains rows of titanium sites with Ti···Ti spacings of 3.78 Å in the rows and 5.12 Å between the rows. The (001) surface has a square unit cell [3.78, 3.78] Å, and thus it does not have a strong anisotropy for anchoring of anions **1**.

As in the case of the N3 complex,[28] we have built only

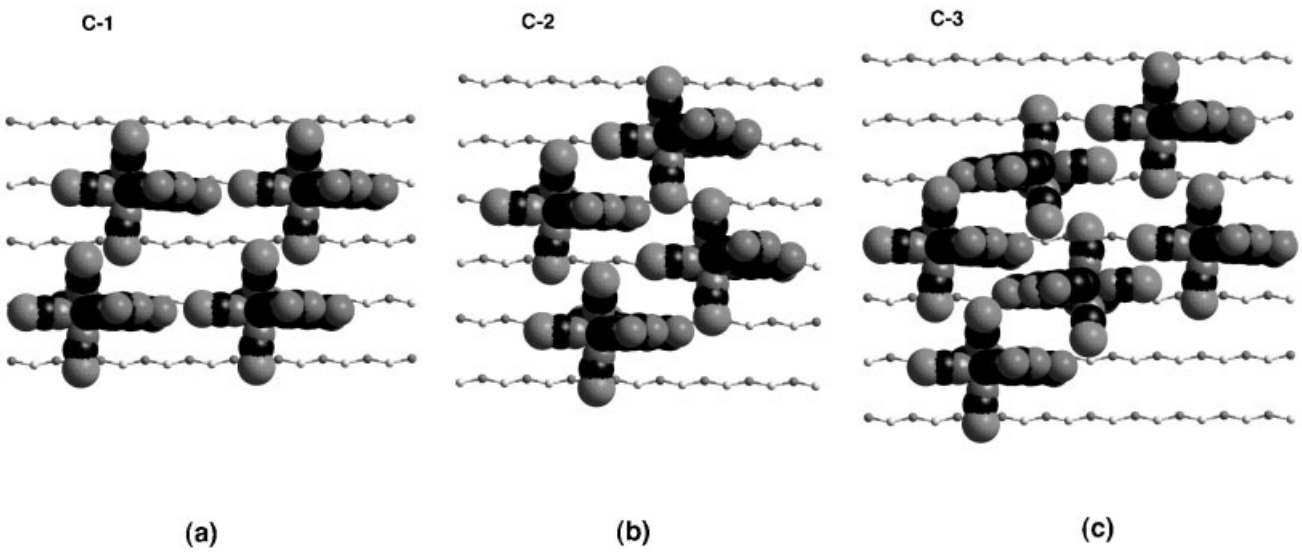

Figure 5. Most-dense regular packings of anions **1** for the C-type of anchoring on the (101) anatase crystal surface. The C-3 unit cell contains two anions of mirror orientation. The surface densities are 0.65, 0.86, and 0.86 molecules/nm^2 for C-1, C-2, and C-3 respectively.

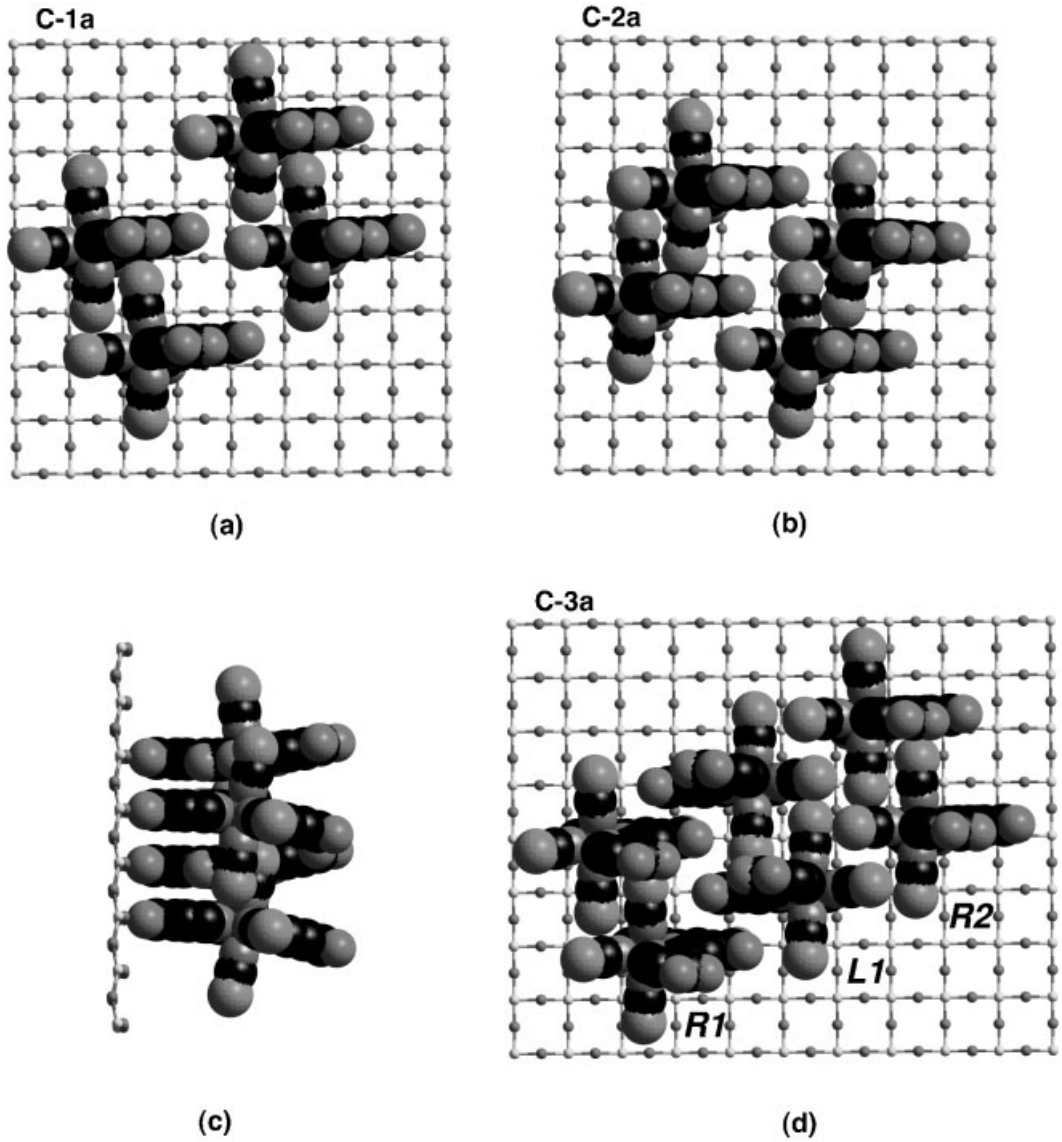

Figure 6. Most-dense regular packings of the C anchoring type on the (001) anatase crystal surface with densities 0.87 (C-1a), 1.00 (C-2a), and 1.17 (C-3a) molecules/nm^2. Mirror *R* and *L* rows in C-3a are to have somewhat different anion inclinations to the TiO_2 surface shown in (c) by side projection.

regular packing models[†] of the adsorbed monolayer with minimal unit cells (one or two molecules per cell). The densest regular packings of anions **1** with C-type anchoring are presented in Figs 5 and 6. Packings of the C-type are significantly more compact than those of the B-type (0.86 versus 0.65 molecules/nm^2 at a maximum for the (101) surface, and 1.17 versus 0.78 molecules/nm^2 at a maximum for the (001) surface), which may be caused by the smaller two-dimensional area of the anion **1** in the C orientation and a larger asymmetry of this molecular projection onto the TiO_2 surface.

The (001) anatase surface, with a more dense and isotropic distribution of chemisorption sites, makes possible more varied and noticeably more compact packing of the anions. This holds for both types of anchoring: the monolayer density maxima increase in comparison with the (101) case by 20% (B-type) and by 36% (C-type).

The experimental value of 0.42 molecules/nm^2 for surface concentration of anions **1** absorbed by the TiO_2 nanocrystal powder[30] is lower than the maximum values found for all the regular packing models described above. A possible reason may be a real irregularity of the monolayer structure

[†]The Serius[2] software (Molecular Simulations Inc., 1997) was used for building interface models.

and, probably, too slow a surface diffusion. However, in any case, the (001) surfaces can accumulate more of anions **1**, and one should increase the coverage (which is rather low)[35] to improve the efficiency of the sensitizer. As to mixed packings of the B and C anchoring types, it is clear that they are most likely irregular and have lower density values than those of the packing types considered.

Two specific types of interaction can significantly affect the monolayer packing: strong H-bonds between anions and their electrostatic interactions within the monolayer. The latter forces are long range and isotropic; therefore, their influence on the short-range order in the absorbed layer cannot be substantial, taking into account that the layer formation proceeds in the presence of cations. On the contrary, the spatial directions of H-bonds are rather strict, and sufficiently intense interactions may exist only within narrow intervals of intermolecular distances, e.g. 2.4–2.6 Å for the O···O spacings. Hence, H-bonds may have a strong influence on the molecular packing.

However, the mutual arrangement of anions **1** in all the models considered above is not favorable for H-bond formation. Moreover, even the assumption of some twisting (up to *ca* 15°) of the anion orientation relative to the state with the minimum steric tension, when the terpyridyl planes are parallel to the rows of surface titanium atoms (see Figs 5 and 6), does not provide hydrogen bonding. Thus, the conclusions made above are applicable equally to irregular structural models. In the case of combinations of the B and C types of anchoring, the conclusions above are also correct, as ensured by the symmetrical geometry of the terpyridyl moiety.

CONCLUSION

The X-ray study of the crystal structure of complex **1** shows the presence of continuous rows of centrosymmetric pairs of molecules in the single crystal, linked into the chains by strong H-bonds. But, according to a molecular modeling study, the formation of H-bonds within the absorbed monolayer onto the (101) and (001) anatase surfaces is unlikely. Nevertheless, the formation hydrogen-bonded ribbons in solution may effectively prevent complex **1** from reaching into the small pores of the TiO_2 surface, causing less efficiency compared with the N3 complex investigated previously. The formation of hydrogen-bonded chains was effectively reduced by decreasing the number of protons from two to one.[30] The TiO_2 electrodes sensitized with complex **1** containing one proton yields a short circuit photocurrent density i_{sc} of 20 mA cm^{-2} and an open circuit potential V_{oc} of 720 mV with a fill factor (ff) of 0.7, yielding an overall solar cell efficiency of 10.4%. These results were confirmed at the National Renewable Energy Laboratory (NREL), Golden, CO, USA. Thus, there can be no question that the overall photovoltaic performance of complex **1** containing one proton supercedes that of the N3 sensitizer due to its superior panchromatic light-harvesting properties.

Supporting information available

Coordinates of atoms, bond lengths, bond angles, anisotropic displacement coefficients, calculated hydrogen atom coordinates, and observed and calculated structure factors are lodged at the Cambridge Crystallographic Data Centre, Cambridge, UK.

Acknowledgements

We are indebted to the Swiss National Science Foundation, Project SCOPES No. 7SUPJ062151.00/1, for financial support. We thank Dr A. McEvoy for his time and discussions.

REFERENCES

1. Siegel RW, Hu E and Roco MC (eds). Nanostructure Science and Technology. A Worldwide Study. WTEC, Loyola College: Maryland, 1999. (http://itri.loyola.edu/nano/final [last accessed: 7 August 2002]).
2. Liu D and Kamat PV. *J. Chem. Phys.* 1996; **105**: 965.
3. Stipkala JM, Castellano FN, Heimer TA, Kelly CA, Livi KJT and Meyer G. *J. Chem. Mater.* 1997; **9**: 2341.
4. Hoyl R, Sotomayor J, Will G and Fitzmaurice D. *J. Phys. Chem. B* 1997; **101**: 10 791.
5. Sanches C and Lebeau B. *MRS Bulletin*. 2001; **26**: 377.
6. Athanassov Y, Rotzinger FP, Pechy P and Grätzel M. *J. Phys. Chem. B* 1997; **101**: 2558.
7. Cusack L, Rizza R, Gorelov A and Fitzmaurice D. *Angew. Chem. Int. Ed. Engl.* 1997; **36**: 848.
8. Rizza R, Fitzmaurice D, Hearne S, Hughes G, Spoto G, Ciliberto E, Kerp H and Schropp R. *Chem. Mater.* 1997; **9**: 2969.
9. Thompson ME. *Chem. Mater.* 1994; **6**: 1168.
10. Ohno K and Kawaoze Y. In *Abstracts of Fifth International Conference on Nanostructured Materials*, 20–25 August, 2000, Sendai, Japan; 170.
11. McEvoy AJ and Grätzel M. *Sol. Energy Mater. Sol. Cells* 1994; **32**: 221.
12. O'Regan B, Moser J, Anderson M and Grätzel M. *J. Phys. Chem.* 1990; **94**: 8720.
13. Kohle O, Ruile S and Grätzel M. *Inorg. Chem.* 1996; **35**: 4779.
14. Taniguchi T and Miyashita T. *Chem. Lett.* 1997; 295.
15. Grunwald R and Tributsch H. *J. Phys. Chem. B* 1997; **101**: 2564.
16. Drago RS, Richardson DE and George JE. *Inorg. Chem.* 1997; **36**: 25.
17. Argazzi R, Bignozzi CA, Heimer TA and Meyer GJ. *Inorg. Chem.* 1997; **36**: 2.
18. Salafsky JS, Lubberhuizen WH, van Faassen E and Schropp REI. *J. Phys. Chem. B* 1998; **102**: 766.
19. Zaban A, Ferrere S and Gregg BA. *J. Phys. Chem. B* 1998; **102**: 452.
20. Pan J-M, Maschhoff BL, Diebold U and Madey TE. *Surf. Sci.* 1993; **291**: 381.
21. Abruna HD, Bommarito GM and Yee HS. *Acc. Chem. Res.* 1995; **28**: 273.
22. Lin W, Lee T-L, Lyman PF, Lee J, Bedzyk MJ and Marks TJ. *J. Am. Chem. Soc.* 1997; **119**: 2205.
23. Granozzi G and Sambi M. *Adv. Mater.* 1996; **8**: 315.
24. Kirstein S and Mohwald H. *Chem. Phys. Lett.* 1992; **189**: 408.
25. Shklover V, Liska P, Nazeeruddin M, Grätzel M, Nesper R and Hermann R. *SPIE Proc. Ser.* 1993; **2017**: 272.

26. Yao X, Ruskell TG, Workman RK, Sarid D and Chen D. *Surf. Sci.* 1996; **367**: L85.
27. Briner BG, Doering M, Rust H-P and Bradshaw AM. *Science* 1997; **278**: 257.
28. Shklover V, Ovchinnikov YuE, Braginsky LS, Zakeeruddin SM and Grätzel M. *Chem. Mater.* 1998; **10**: 2533.
29. Finnie KS, Bartlett JR and Woolfrey JL. *Langmuir* 1998; **14**: 2744.
30. Nazeeruddin MdK, Pechy P, Renouard T, Zakeeruddin SM, Hamphry-Baker R, Comte P, Liska P, Cevey L, Costa E, Shklover V, Spiccia L, Deacon GB, Bignozzi CA and Grätzel M. *J. Am. Chem. Soc.* 2001; **123**: 1613.
31. Sheldrick GM. *SHELXTL PC Version 5.0. An Integrated System for Solving, Refining, and Displaying Crystal Structures from Diffraction Data*. Siemens Analytical X-Ray Instruments, Inc.: Madison, WI, 1994.
32. Leiserowitz L. *Acta Crystalliogr. Sect.s'* 1976; **32**: 775.
33. Jeffrey GA. *An Introduction to Hydrogen Bonding*. Oxford University Press: New York, 1997; 2.
34. Hengerer R, Bolliger B, Erbudak M and Gratzel M. *Surf. Sci.* 2000; **460**: 162.
35. Shklover V, Haibach T, Bolliger B, Hochstrasser M, Erbudak M, Nissen H-U, Zakeeruddin SM, Nazeeruddin MdK and Gratzel M. *J. Solid State Chem.* 1997; **132**: 60.
36. Shklover V, Nazeeruddin MdK, Zakeeruddin SM, Barbe C, Kay A, Haibach T, Steurer W, Hermann R, Nissen H-U and Grätzel M. *Chem. Mater.* 1997; **9**: 430.
37. Wang L-Q, Ferris KF, Shultz AN, Baer DR and Engelhard MH. *Surf. Sci.* 1997; **380**: 352.

